

Antigen presenting cells expressing Fas ligand down-modulate chronic inflammatory disease in Fas ligand-deficient mice

Huang-Ge Zhang,¹ Martin Fleck,² Earl R. Kern,³ Di Liu,¹ Yongming Wang,¹ Hui-Chen Hsu,¹ Pingar Yang,¹ Zheng Wang,¹ David T. Curiel,⁴ Tong Zhou,¹ and John D. Mountz^{1,5}

¹Department of Medicine, Division of Clinical Immunology and Rheumatology, University of Alabama-Birmingham, Birmingham, Alabama 35294, USA

²Department of Medicine, The University of Regensburg, Regensburg, Germany

³Department of Microbiology, and

⁴Gene Therapy Program, University of Alabama-Birmingham, Birmingham, Alabama 35294, USA

⁵Veterans Administration Medical Center, Birmingham, Alabama 35233, USA

Address correspondence and reprint requests to: John D. Mountz, University of Alabama at Birmingham, Department of Medicine, Division of Clinical Immunology and Rheumatology, 701 South 19th Street, LHRB 473, Birmingham, Alabama 35294, USA. Phone: (205) 934-8909; Fax: (205) 975-6648; E-mail: john.mountz@ccc.uab.edu.

Received for publication August 23, 1999, and accepted in revised form January 31, 2000.

We assessed the effect of modified antigen presenting cells (APCs) expressing high levels of Fas ligand (APC-FasL) on post-viral chronic inflammatory disease. FasL-deficient B6-*gld/gld* mice infected with murine cytomegalovirus (MCMV) cleared the virus from their lungs, kidneys, and livers within 2 weeks of infection. However, inflammation persisted in these organs for more than 8 weeks, with a chronically increased T-cell response to MCMV-infected APCs and production of autoantibodies. Administration of APC-AdFasL at 4 weeks suppressed this inflammation and diminished the T-cell response and autoantibody production. APC-AdFasL that had been transfected with ultraviolet-irradiated MCMV were more effective than uninfected APC-AdFasL in ameliorating the chronic inflammation. APC-AdFasL migrated preferentially to the spleen, where they triggered apoptosis of lymphocytes in the marginal zone of the spleen. These results confirm that Fas-mediated apoptosis is not required for clearance of virus, but is required for down-modulation of the virally induced chronic inflammatory response. This organwide effect of APC-AdFasL appears to be mediated by elimination of activated T lymphocytes in the spleen before their emigration to the target organs.

J. Clin. Invest. 105:813–821 (2000).

Introduction

Activation-induced cell death (AICD) down-modulates the immune response (1–5) and, therefore, plays a key role in the prevention of inflammatory and autoimmune responses. AICD of T cells, B cells, and macrophages is mediated by Fas (APO-1/CD95), which is a member of the TNF-receptor superfamily (6–8). Elucidation of the physiological effects of Fas/FasL signaling has been facilitated greatly by the identification of the spontaneous mutation of the *fas* gene in *lpr/lpr* mice (9–12) and of the *fas ligand* gene in *gld/gld* mice (13, 14). Homozygous expression of either of these mutant genes leads to lymphoproliferation and systemic autoimmune disease with autoantibody production, nephritis, vasculitis, and arthritis (15, 16).

To determine the role of Fas-mediated apoptosis in the inflammatory sequelae of viral infections, we previously characterized the development of chronic inflammatory disease in 4-week-old Fas-deficient B6-*lpr/lpr* mice infected with murine cytomegalovirus (MCMV) (17, 18). The initial inflammatory response and viral clearance in the mutant mice were nearly equivalent to that in the wild-type mice, and, by 3–4 weeks after infec-

tion, the MCMV virus was not detectable in the lung, kidney, or liver of either the mutant or wild-type mice. The MCMV-infected wild-type mice did not exhibit any persistent sequelae of the infection. In contrast, the MCMV-infected B6-*lpr/lpr* mice developed a chronic inflammation of the lung, kidney, and liver that was associated with production of anti-ds-DNA autoantibodies and rheumatoid factor (RF), symptoms that are not apparent in uninfected B6-*lpr/lpr* mice of the same age. These studies indicated that interaction between Fas and FasL is not required for effective clearance of virus but is required for subsequent down-modulation of the immune response to the virus. The failure of this down-modulation in Fas-mediated apoptosis defective mice provides a model of virally induced chronic inflammation and autoimmune disease.

The fundamental role of Fas-mediated apoptosis in regulation of apoptosis suggests that enhancement of this response may be effective in the prevention and treatment of chronic inflammatory and autoimmune conditions. Administration of APCs that have been modified to express high levels of FasL may be particularly effective in down-modulating T-cell responses (19). Therefore, we

have characterized the effect of administration of appropriately modified APCs in normal mice. APCs that have been modified to express FasL and adenovirus (APC-AdFasL) migrate predominantly to the spleen, resulting in the elimination of T cells that specifically recognize antigens expressed by the APCs (20). Thus, administration of APC-AdFasL results in specific AICD of those T cells capable of responding to the adenovirus (21). Elimination of the virally reactive T cells resulted in a decreased immune response to administration of the virus during the lifetime of the modified APCs.

In this study, we further characterized the role of Fas-mediated apoptosis in the chronic inflammatory sequelae of viral infection by extending the model to FasL-deficient *gld-gld* mice and used this model to determine whether FasL-modified APCs can be used to modulate this response. Young $B6^{+/+}$ mice and $B6-gld/gld$ mice were inoculated intraperitoneally with MCMV, and APC-AdFasLs were administered intravenously 4 weeks later. To determine the requirement for MCMV antigen presentation by APC-AdFasL, separate groups of mice were treated with APC-AdFasL that were transfected with ultraviolet-irradiated (UV-irradiated) MCMV. The results indicate that both MCMV-infected and uninfected APC-AdFasL are highly effective in down-modulating the inflammatory response after MCMV infection, by inducing apoptosis of lymphocytes in the marginal zone of the spleen. These results support the concept that the post-MCMV inflammatory disease of the lung, kidney, and liver in $B6-gld/gld$ mice is due to continued migration of splenic lymphocytes to these organs, with subsequent entry and activation at these sites.

Methods

Animals. Six- to 10-week-old female $B6^{+/+}$, $B6-gld/gld$, and $B6-lpr/lpr$ mice were obtained from The Jackson Labo-

ratories (Bar Harbor, Maine, USA) and were maintained in our own certified animal facility at the University of Alabama at Birmingham under pathogen-free conditions.

Virus and virus titration. As described previously (18), female Balb/c mice were inoculated intraperitoneally with MCMV strain Smith obtained from the American Type Culture Collection (Rockville, Maryland, USA), and salivary glands were collected 12 days later. The salivary glands were homogenized in DMEM (GIBCO BRL, Grand Island, New York, USA) containing 10% FBS and centrifuged. The supernatant was dispensed into aliquots, which were stored at -80°C and used as the MCMV stock virus pool (3×10^7 plaque-forming units [pfu] per milliliter). For the determination of the virus titer in tissues, organs were removed and homogenized as 10% (wt/vol) suspensions in DMEM (GIBCO BRL) supplemented with L-glutamine, 10% FCS penicillin/streptomycin, and amphotericin B. The homogenates were titrated as duplicates in \log_{10} dilutions on subconfluent primary murine embryo fibroblasts in 12-well plates. Seven days later, the monolayers were stained with neutral red and the number of plaques counted.

Histological assessment and immunophenotyping. As described previously (18), organs were removed and fixed in 10% phosphate-buffered formalin. After paraffin embedding, tissue sections were cut ($5\ \mu\text{m}$) and stained with hematoxylin and eosin (H&E) for morphological evaluation. Histopathological scoring was performed by rating the severity of lesions and infiltration on a scale from 0 to 4. The following criteria were applied for the grading scale: 0, normal histology; 1, minimal mononuclear cell infiltration with or without minimal cell destruction; 2, modest mononuclear cell infiltration with 1–2 clear foci per field of view with focal cellular destruction; 3, numerous aggregates (3–5) of mononuclear cells per field of view with destruction of lung, kidney, or liver tissue at several locations; and 4, severe infiltration with mononuclear cells in multiple foci per lobe with destruction of lung, kidney or liver tissue. The histopathology was scored by 3 observers blinded to the treatment protocol, and the score represents the mean, with error bars representing the SEM.

For immunochemistry, the organs were removed and fixed in neutral 10% formalin/PBS

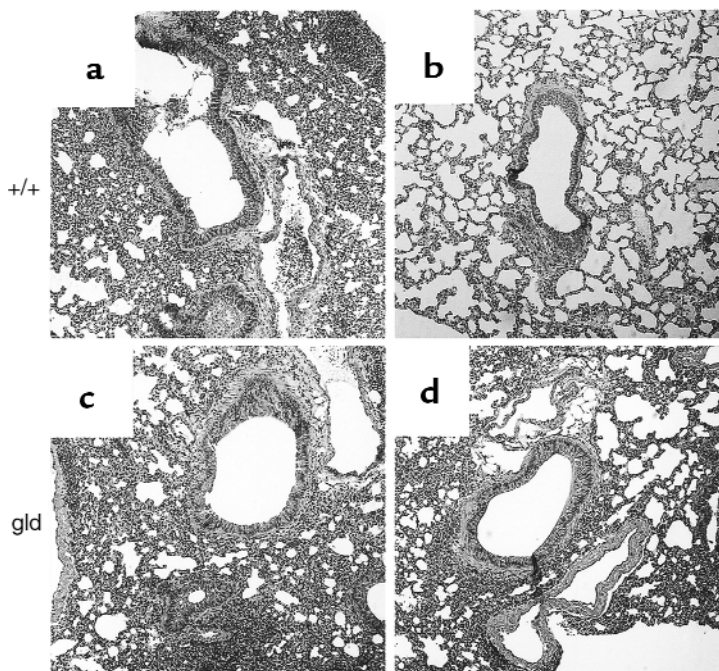


Figure 1

MCMV-induced chronic disease in the lungs of $B6-gld/gld$ mice. $B6^{+/+}$ and $B6-gld/gld$ mice were inoculated intraperitoneally with MCMV (105 pfu). Histological examination of the lungs was performed ($\times 40$) at day 7 (**a, c**) and day 28 (**b, d**) after infection. The severe acute chronic inflammatory response in both $B6^{+/+}$ and $B6-gld/gld$ mice was characterized by interstitial pneumonitis (**a, c**), which persisted in $B6-gld/gld$ (**d**) but not $B6^{+/+}$ mice (**b**).

for 24 hours, followed by fixation in 70% ethanol for 24 hours. After paraffin embedding, tissue sections were cut (10 μm) and stained with H&E before deparaffinization and treatment with 3% H_2O_2 at room temperature for 15 minutes. After washing 3 times with neutral PBS, tissues were first incubated with a mAb specific for CD3 (DAKO Corp., Carpinteria, California, USA) following standard avidin-biotin conjugate (ABC) immunohistochemical techniques according to the manufacturer's manual. A peroxidase-conjugated secondary antibody was then applied to the sections at room temperature for 2 hours. Positive staining was viewed using diaminobenzidine (DAB) substrate (Dako Corporation). Apoptosis analysis of the liver by Hoechst staining was carried out using a 1:2,000 dilution of stock Hoechst (600 $\mu\text{g}/\text{mL}$ dissolved in PBS) as described previously (20).

Terminal deoxyribonucleotidyl transferase-mediated dUTP nick end labeling. The method was modified slightly from that described previously (18). In brief, formalin-fixed and paraffin-embedded tissue sections were deparaffinized and rehydrated. After thorough washing with deionized water, the tissue sections were subjected to permeabilization with proteinase K (10 $\mu\text{g}/\text{mL}$ at room temperature for 15 minutes) and then incubated with freshly prepared terminal deoxyribonucleotidyl transferase (TDT) reaction mix (0.4 u/L TDT, 10 nM digitonigen modified-dUTP, and TDT buffer, which were purchased from Boehringer Mannheim, Indianapolis, Indiana, USA) at 37°C for 60 minutes. The incorporated digitonigen-dUTP was detected by incubation with AP-conjugated anti-digitonigen antibody at room temperature for 60 minutes, and positive reactions were revealed using NBT/BCIP (nitroblue tetrazolium chloride/5-bromo-4-chloro-3-indolyl phosphate) substrate. Methyl green was used for counterstaining.

Quantitation of autoantibodies. Serum levels of anti-double-strand (ds) DNA antibodies and rheumatoid factor (RF) were determined by sandwich ELISA as described previously (18). Sera samples were obtained from 5 mice per group of uninfected and infected mice. In brief, for quantitation of anti-dsDNA antibodies, 96-well microtiter plates were precoated with 10 $\mu\text{g}/\text{mL}$ of poly-L-lysine followed by 10 $\mu\text{g}/\text{mL}$ of dsDNA or 10 $\mu\text{g}/\text{mL}$ of poly-L-glutamic acid as background control. For detection of RF, 96-well microtiter plates were coated with 4 $\mu\text{g}/\text{mL}$ of affinity-purified rabbit IgG (all reagents were obtained from Sigma Chemical Co., St. Louis, Missouri, USA). The sera were diluted at 1:100 and incubated at room temperature for 4 hours. Bound anti-dsDNA antibodies or RF was detected by an IgG isotype-specific alkaline phosphatase-conjugated goat anti-mouse Ig (PharMingen, San Diego, California, USA). *P*-nitrophenylphosphate (Sigma Chemical Co.) was used as substrate, and the color development was measured at 405 nm using an Emax microplate reader (Molecular Devices, Menlo Park, California, USA).

Construction of Fas ligand expression adenovirus vector. As described previously (19), the 1.6-kb chicken β -actin promoter plus the CMV enhancer was cloned into a 10.4-kb

shuttle vector containing the fragment of adenovirus from 0 map units to 1 map units. Two *Loxp* sites separated by a Neo-resistant gene plus a 0.3-kb bovine growth hormone poly A tail was cloned downstream of this promoter/enhancer. The full-length 0.9-kb FasL was cloned downstream from the bovine growth hormone poly A tail that was followed by an SV40 poly A tail and by the 9.8–16.1 map unit region of adenovirus.

Adenovirus growth and titration. Stock virus was inoculated into 293 cells. After 36 hours, the infected cells were lysed by 3 freeze/thaw cycles. The virus released into the supernate was loaded onto a triple-layer cesium chloride gradient of 1.5 g/mL, 1.4 g/mL, and 1.2 g/mL. The virus was banded using a SW41 rotor at 89,000 g at 4°C for 18 hours. The virus band was removed and dialyzed against PBS + 10% glycerol (pH 7.4) for 12 hours at 4°C. Then the virus was aliquoted and frozen at -90°C until use. The virus titer was quan-

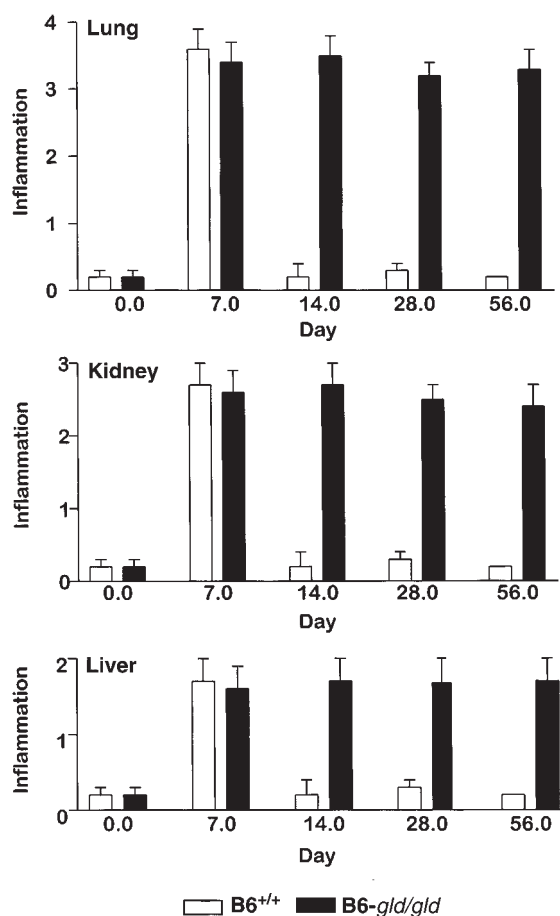
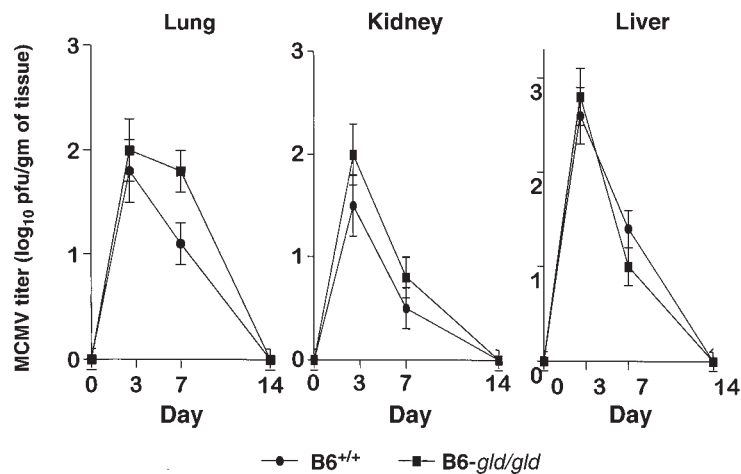


Figure 2

Quantitative analysis of inflammation in the lung, kidney, and liver. B6^{+/+} and B6-gld/gld mice were infected intraperitoneally with MCMV (1×10^5 pfu) and lung (top panel), kidney (middle panel), and liver (bottom panel) tissues were assessed for severity of inflammation and tissue damage on a relative scale ranging from 0 (not present) to 4 (most severe). The bar graph represents the score \pm SEM of at least 5 mice analyzed at each time point.

Figure 3

Efficient clearance of MCMV virus in B6-*gld/gld* mice. Quantitation of infectious MCMV in the lung, kidney, and liver of B6^{+/+} and B6-*gld/gld* mice was performed at different time points using a plaque assay. The values represent the mean ± SEM from different tissue of at least 3 mice analyzed at each time point.



titated using a standard plaque-forming assay in 293 cells. Quality control of the virus was carried out by biologic functional analysis (19). This includes the ability of the AdLoxP FasL plus AdCre to induce high levels of Fas ligand capable of inducing apoptosis of A20 target cells. As a control, AdLoxPFasL was added with AdLacZ to ensure that no Fas ligand was produced by the AdLoxPFasL vector in the absence of AdCre.

Infection of APCs for FasL expression. An APC cell line was derived from *lpr/lpr* mice, as described previously (20). This APC cell line exhibited high expression of Mac-1, CD28, and class II MHC. The APCs were transfected with the AdLoxPFasL plus AxCANCre, and Fas ligand cell-surface expression was characterized by flow cytometry using an anti-FasL antibody (clone Kay-10; PharMingen) as described previously. Greater than 50% of APCs expressed high levels of FasL. For experiments described in this article, these Fas-deficient murine B6-*lpr/lpr* APCs were infected with either AdLoxPFasL plus AxCANCre (APC-AdFasL) or AdCMVLacZ (APC-AdLacZ) at 5 pfu/cell of each virus for 1 hour at 37°C as described previously (19). For some experiments, the APCs were also infected with UV-irradiated MCMV (APC+MCMV or APC-AdFasL+MCMV) (5 pfu/cell). The APCs were then washed, and the infected cells were incubated at 37°C for an additional 24 hours. Expression of murine FasL and adenoviral antigens on the surface of B6-*lpr/lpr* APCs was identified using an indirect immunofluorescent assay, and the ability of FasL to mediate killing was evaluated using a [⁵¹Cr] release assay as described previously (21).

Administration of APC-AdFasL. Eight-week-old B6^{+/+} and B6-*gld/gld* mice were injected intravenously every 3 days for 5 doses with 1 × 10⁶ of either APCs coinfecting with AdLoxPFasL plus AxCANCre (APC-AdFasL) or APCs coinfecting with AdCMVLacZ (APC-AdLacZ). For some experiments, mice were treated with APCs that were also infected with UV-irradiated MCMV (APC-AdFasL+MCMV) (5 pfu/cell). As a control, mice were treated with APCs that were only infected with UV-irradiated MCMV (APC+MCMV). All mice were sacrificed 4 weeks after treatment with APC-AdLacZ, APC-MCMV, APC-AdFasL, and APC-AdFasL+MCMV.

Localization of APC-AdCMVGFP. APC-AdCMVGFP were produced using an adenovirus shuttle vector and recombination with Ad genome. B6^{+/+} mice were injected intravenously with 1 × 10⁶ APC-AdCMVGFP or control APCs (5 mice per group). Mice were sacrificed 48 hours later, and frozen sections of the liver and spleen were analyzed by fluorescence microscopy (×80).

In vitro IL-2 production. APCs from B6^{+/+} mice were infected with UV-irradiated MCMV for 1 hour in 1 mL of media and then diluted by addition of 10 mL of RPMI 1640 supplemented with 10% FBS and culture continued at 37°C for 24 hours. Before use as stimulator cells, the APCs were γ-irradiated, and 1 × 10⁵ APCs were mixed with T cells isolated from the spleen of APC-AdFasL-treated, APC-AdFasL+MCMV-treated, and APC-AdLacZ-treated mice. The mixed cells were incubated in 96-well plates for 2 days at 37°C. The supernatants were collected and induction of IL-2 was determined using an ELISA assay kit (R&D Systems Inc., Minneapolis, Minnesota, USA).

Statistical analysis. The 2-tailed Student's *t* test was used for statistical analysis when 2 different groups of samples were compared. The 1-factor ANOVA test was used when more than 2 groups of samples were compared. A *P* value of less than 0.05 was considered significant.

Results

Chronic inflammatory response in the lung, kidney, and liver of MCMV-infected B6-*gld/gld* mice. We have shown previously that infection of B6-*lpr/lpr* mice with MCMV induces the development of a chronic inflammatory response, characterized by pneumonitis, nephritis, and hepatitis that persists for 100 days despite clearance of infectious MCMV by day 28 (17, 18). A similar chronic inflammatory disease was observed in the lung, kidney, and liver of B6-*gld/gld* mice after infection with MCMV. Histological examination performed 7 days after infection by intraperitoneal injection with MCMV (1 × 10⁵ pfu) revealed an acute inflammatory response in the lungs of both the B6^{+/+} and B6-*gld/gld* mice (Figure 1, a and c). In both strains of mice, the interstitial pneumonitis was evidenced by the high number of lymphocytes in the parabronchial and interstitial regions. After 4 weeks, the inflammation had resolved in the lungs of

the B6^{+/+} mice, but was still evident in those of the B6-*gld/gld* mice (Figure 1, b and d).

A severe inflammatory response was observed in the kidney and liver, as well as the lungs of the MCMV-infected B6-*gld/gld* mice, and this persisted for more than 56 days after infection (Figure 2). The manifestations of the interstitial pneumonitis in these mice on day 56 resembled those seen on day 28 except that in the chronic inflammatory response, the typical features included thickening of the alveolar septa, hyperplasia of alveolar macrophages, and paravascular and parabronchial lymphocytic infiltration (Figure 2a). Proliferative glomerulonephritis with multifocal tubular degeneration and a lymphocytic infiltration in the interstitium indicated a chronic nephritis (Figure 2b). The chronic hepatitis was characterized by a moderate number of multifocal infiltrates of mononuclear cells as well as degeneration and regeneration of hepatocytes (Figure 2c). These features indicate a chronic inflammatory response, and their occurrence in MCMV-infected B6-*gld/gld* mice, but not B6^{+/+} mice or uninfected B6-*gld/gld* mice of the same age, indicates that Fas-mediated apoptosis is required for the down-modulation of the inflammatory response induced by MCMV.

Viral clearance in MCMV-infected mice. We have established previously that MCMV is cleared rapidly from the lung, kidney, and liver of B6-*lpr/lpr* as well as B6^{+/+} mice (18). To determine whether MCMV also was cleared rapidly from the lung, kidney, and liver of B6-*gld/gld* mice, infective MCMV was quantitated in these organs at different time points using a plaque assay. Clearance of

MCMV was rapid and effective in the lung, kidney, and liver, and, by day 14, MCMV was no longer detectable in any organs in either strain of mouse (Figure 3). Therefore, the chronic inflammatory response that was observed in the lung, kidney, and liver of B6-*gld/gld* mice was not due to persistent infection by MCMV.

Administration of APC-AdFasL ameliorates inflammation after MCMV infection in B6-*gld/gld* mice. To determine the effect of APC-AdFasL treatment, B6-*gld/gld* mice were first inoculated intraperitoneally with MCMV (1×10^5 pfu), which induced the chronic inflammatory response already described here. At 4 weeks after MCMV infection, the mice were injected intravenously with either 1×10^6 APC-AdFasL (APC+FasL) or 1×10^6 control APC-AdCMVLacZ (APC). On sacrifice and analysis 4 weeks later, the inflammatory response in the lungs of mice treated with APC-AdFasL was much less severe than that in the lungs of mice treated with APC-AdCMVLacZ (Figure 4). The less-severe inflammatory response was associated with a lower number of infiltrating CD3⁺ T cells as determined by immunohistochemical staining (Figure 4).

We have demonstrated previously that adenovirus-pulsed APCs that express FasL (APC-AdFasL) can induce apoptosis of adenovirus-specific T cells and result in specific suppression of the T-cell response to adenovirus (21). Therefore, we determined whether the inflammatory immune response after MCMV infection could be more effectively down-modulated by treatment with APC-AdFasL+MCMV. The APC-AdFasL were first transfected with UV-irradiated MCMV (5 pfu/cell); then $1 \times$

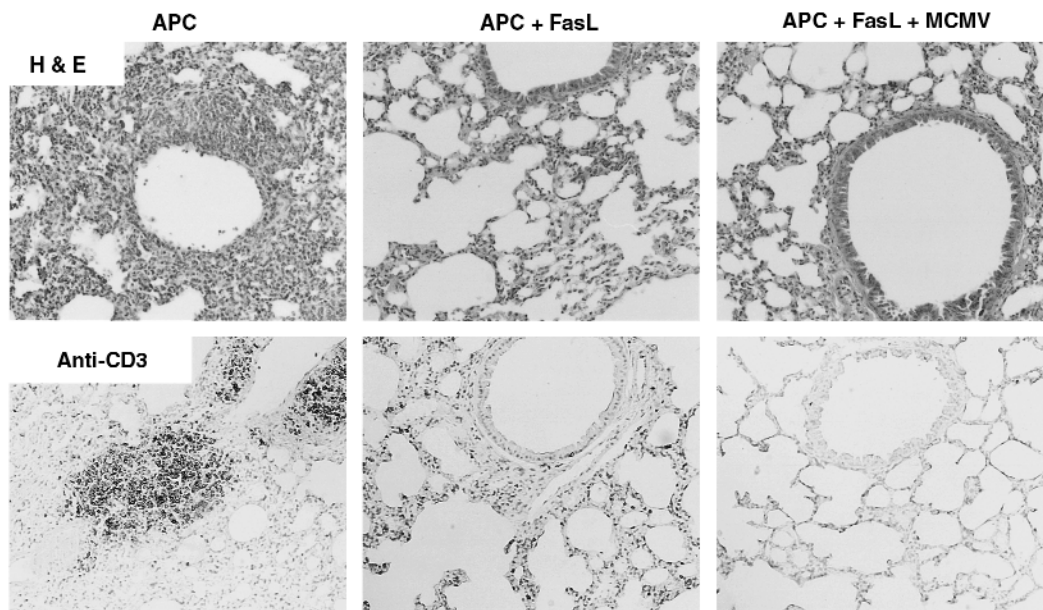


Figure 4

Administration of APC-AdFasL results in less-severe chronic inflammation and lower numbers of T cells in the lungs of MCMV-infected B6-*gld/gld* mice. Four weeks after MCMV infection, B6-*gld/gld* mice were treated with 10^6 of either APC-AdCMVLacZ (APC), 10^6 of APC-AdFasL, or 10^6 of APC-AdFasL+MCMV. APC-AdFasL+MCMV was produced by infection of APC-AdFasL with UV-irradiated MCMV (5 pfu/cell). Four weeks later, the mice were sacrificed and sections were examined after H&E stain and after staining with anti-CD3. A representative photograph ($\times 10$) of a mouse from each group is shown. There were at least 5 mice in each treatment group.

10⁶ of the APC-AdFasL+MCMV was injected intravenously into B6-*gld/gld* mice 28 days after MCMV infection. The inflammatory response in the lungs of mice treated with APC-AdFasL+MCMV was even lower than that of mice treated with APC-AdFasL (Figure 4).

Gradation of the severity of inflammation on a scale of 0 (not present) to 4 (most severe) indicated that the inflammatory response after infection in the lungs, kidney, and liver was significantly less severe in B6-*gld/gld* that were treated with APC-AdFasL compared with untreated mice, whereas a statistically significant difference was not achieved when mice were treated with control APC-AdCMVLacZ (Figure 5). The inflammatory response in the lungs, kidney, and liver of mice treated with APC-AdFasL+MCMV was even lower than that of mice treated with APC-AdFasL (Figure 5). The decreased inflammatory response required Fas expression, as there was no significant decrease in the inflammatory response in B6-*lpr/lpr* mice treated with APC-AdFasL or APC-AdFasL+MCMV 28 days after MCMV infection (Figure 5). Likewise, there was no apoptosis in the spleen of B6-*lpr/lpr* mice after treatment with APC-AdFasL or APC-AdFasL+MCMV (data not shown). The decreased inflammatory response also required Fas ligand expression by the APCs, as there was no significant decrease in the inflammatory response in B6-*gld/gld* mice treated with APC+MCMV 28 days after MCMV infection (Figure 5).

Apoptosis in the spleen of APC-AdFasL-treated B6-gld/gld mice. Although intravenous administration of APCs results in migration predominately to the spleen of the mice (21), intravenous administration of adenovirus targets the liver (22). We have found that intravenous administration of AdCMVLoxp + AxCANCre results in extensive FasL-mediated apoptosis in the liver, which precipitates the death of the animal (19). Therefore, it was important to determine the migration pattern of the APC-AdFasL after intravenous administration. B6-*gld/gld* mice were treated with either 1 × 10⁶ APC-AdCMVGFP or 1 × 10⁶ APC-AdFasL, and the lung, kidney, liver, and spleen were harvested 2 days later for analysis of GFP expression and analysis of apoptosis using the TDT-mediated dUTP nick end labeling (TUNEL) method.

To determine whether APC-adenovirus gene therapy is expressed in the spleen, the migration of APCs after transfection with Ad was monitored using APC-AdCMVGFP. GFP expression by the APC-AdCMVGFP was predominantly in the marginal zone of the spleen (Figure 6a). There was no evidence of migration of APC-AdCMVGFP to the liver (Figure 6d). There was also no detectable migration of APC-AdCMVGFP to the lung or kidney (data not shown). These results confirm that intravenous administration of the APC-AdCMVGFP targets the spleen and not the lung, kidney, or liver.

To verify that apoptosis of mononuclear cells that colocalized with CD3⁺ T was present in the spleen but not apparent in the liver after administration of APC-

AdFasL, spleen and liver were analyzed for apoptosis 2 days after administration of APC-AdFasL by TUNEL staining and Hoechst staining, respectively. There was extensive apoptosis of mononuclear cells in the marginal zone of the spleen (Figure 6c). This distribution of apoptosis staining correlated with immunohistochemical staining with anti-CD3. (Figure 6b). In contrast, there was no apoptosis of liver cells as determined by Hoechst staining (Figure 6e). Neither was there significant apoptosis of mononuclear cells or parenchymal cells in the lung and kidney (data not shown). These results suggest that the APC-AdFasL migrate predominantly to the spleen, where FasL is expressed and T cells are induced to undergo apoptosis. They also suggest a mechanism of action in which the reduction in the inflammatory response in the lung, kidney, and liver is incurred through deletion of lymphocytes in the marginal zone of spleen by the APC-AdFasL; thus, lymphocytes that would normally emigrate from the spleen to target organs are eliminated.

Reduction of MCMV-reactive T cells in vivo. To determine whether the apoptosis of splenic T cells results in a reduced number of MCMV-reactive T cells in vivo, spleen cells were isolated from mice 4 weeks after treatment with APC-AdFasL, APC-AdFasL+MCMV, or control APC-AdCMVLacZ. The T cells were stimulated in vitro with MCMV-pulsed APCs from B6 mice, and the supernatant was harvested 48 hours later. The T cells obtained from mice treated with the APC-AdCMVLacZ control responded with production of high levels of IL-2 (Figure 7); this response was lower in the T cells of

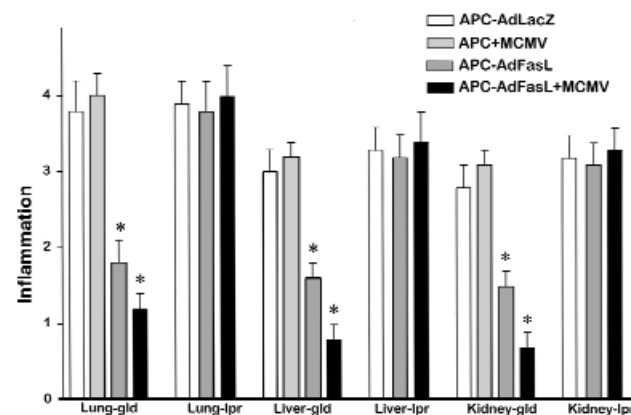


Figure 5 Less-severe inflammation in the lung, kidney, and liver of APC-AdFasL-treated MCMV-infected B6-*gld/gld* mice. B6-*gld/gld* and B6-*lpr/lpr* mice were treated with either APC-AdCMVLacZ (control), MCMV-infected APC (APC+MCMV), APC-AdFasL, or APC-AdFasL+MCMV beginning 28 days after MCMV infection. The mice were treated every 3 days with 4 doses and analyzed 4 weeks after initiation of APC therapy. There were at least 5 mice in each treatment group. The lung, kidney, and liver were stained for H&E and scored by 3 blinded investigators. The histology score was as described in Figure 2. At least 10 fields of view were analyzed for each organ of each mice. The bar graph represents the mean ± SEM of the inflammatory scores from each organ for mice underlying the indicated treatment. *P < 0.05, compared with control treatment group.

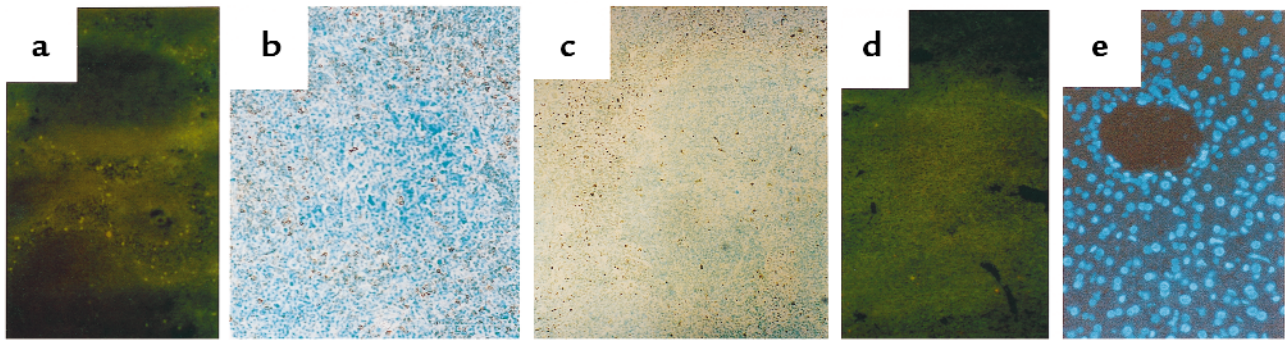


Figure 6

Higher levels of apoptosis in APC-AdFasL–treated B6-*gld/gld* mice after MCMV infection. B6-*gld/gld* mice were treated with either 10^6 APC-AdFasL or 10^6 APC-AdGFP expression, and lung, kidney, liver, and spleen were harvested 2 days later and analyzed for cell localization by fluorescent microscopy (a, d). Apoptosis was determined by the TUNEL method (c) and Hoechst staining (e). T cells were analyzed by immunohistochemical staining with Fitc-anti CD3 (b).

mice treated with APC-AdFasL and lowest in T cells obtained from mice treated with APC-AdFasL+MCMV. These results indicate that APC-AdFasL and APC-AdFasL+MCMV therapy depletes those T cells that are capable of reacting with MCMV when presented by APCs from B6 mice.

Decreased autoantibody production after administration of APC-AdFasL. The production of anti-dsDNA and RF on day 28 after MCMV infection was higher in B6-*gld/gld* mice than in wild-type mice. Analysis of sera obtained 4 weeks after treatment with APC-AdFasL, APC-AdFasL+MCMV, or control APC-AdCMVLacZ indicated that the levels of IgG1, ds-DNA, and IgG1 RF were significantly lower in the sera of mice treated with APC-AdFasL than those treated with control APC-AdCMVLacZ (Figure 8). The levels of these autoantibodies were even lower after treatment with APC-AdFasL+MCMV. These results indicate that autoantibody production is associated with the chronic inflammatory response after MCMV infection and that treatment with APC-AdFasL or MCMV-infected APC-AdFasL can down-modulate the production of autoantibodies.

Discussion

A molecular model that fully accounts for the establishment of chronic inflammation after clearance of a viral infection has not been established. One mechanism that may contribute to the chronic response may be inefficient initial clearance of the virus. Apoptosis of virally infected cells has been recognized as a critical mechanism by which the host limits virus spread, and the presence of apoptotic cells has been reported during several viral infections, including MCMV (23, 24). However, we have previously shown that viral clearance is not defective in B6-*lpr/lpr* mice, and the present results indicate that MCMV viral clearance also is normal in B6-*gld/gld* mice (18). Thus, Fas-mediated apoptosis is not a limiting factor in viral clearance and is not the underlying cause of the persistent inflammation exhibited by the MCMV-infected B6-*gld/gld* mice. These

results are consistent with previous observations in another model of postviral inflammation in which coxsackie virus B1 induces chronic inflammatory myopathy in B6 mice (25). Although different strains of B6 mice show variable degrees of susceptibility to postviral inflammatory myopathy, the efficiency of viral clearance is not a determining factor.

Our previous results indicated that down-modulation of the immune response after clearance of MCMV is mediated by Fas-FasL interactions (17, 18). The present study indicates that in the absence of FasL in B6-*gld/gld* mice, an inflammatory response persists after clearance of the virus. Histological examination of the lung, kidney, and liver at different time points after MCMV infection revealed a severe, chronic inflammatory disease in B6-*gld/gld* mice, which was characterized by large numbers of infiltrating T cells. Because chronic disease did not develop in MCMV-infected B6^{+/+} mice, it can be concluded that Fas-FasL interactions are required for down-modulation of an inflammatory response after the clearance of virus. Down-modulation of the inflammatory response requires expression of Fas, as the inflammatory response in MCMV-infected B6-*lpr/lpr* mice (18) cannot be down-modulated by treatment with APC-AdFasL or APC-AdFasL+MCMV. Down-modulation of the inflammatory response requires expression of Fas ligand by the APC, as the inflammatory response in MCMV-infected B6-*gld/gld* mice cannot be down-modulated by treatment with APC+MCMV. Excessive inflammation was not due to a persistent infection in B6-*gld/gld* mice, as the clearance of MCMV was not delayed and no infectious MCMV could be detected in the lung, kidney, and liver of these mice at day 14. Taken together, our studies strongly implicate defects in FasL and Fas-mediated apoptosis in predisposition to chronic postviral inflammatory disease processes.

The current results utilized APCs transfected with AdLoxpFasL plus AxCANCre to achieve very high levels of FasL expression in almost 100% of infected APCs (20, 21). The high efficiency of FasL expression accomplished by this technique is due, in part, to the very

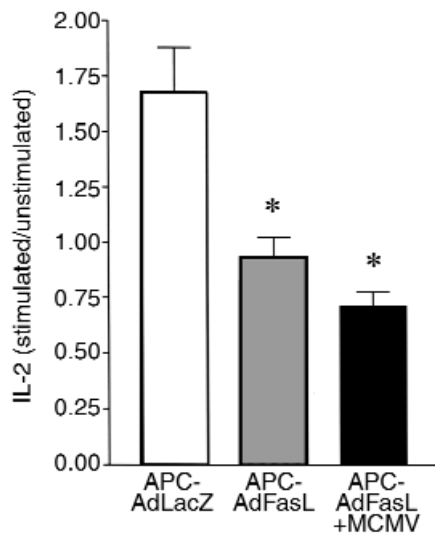


Figure 7

Percentage of MCMV-reactive T cells in vivo. Spleen cells were isolated from MCMV-infected mice 4 weeks after treatment with APC-AdLacZ control, APC-AdFasL, or APC-AdFasL+MCMV. T cells were stimulated in vitro with MCMV pulse APCs from B6-*lpr/lpr* mice, and the supernate was harvested 48 hours later. * $P < 0.05$, compared with control treatment group.

high titers of both viruses in the 293 cells resulting from the lack of FasL expression by AdLoxpFasL, which requires co-infection with a AxCANCre virus (19). In addition, this two-virus system was used to infect an APC cell line derived from B6-*lpr/lpr* mice; consequently, these APCs can express high levels of FasL without undergoing autocrine suicide. Extremely efficient inhibition of CD3⁺ T-cell by APC-AdFasL after adenovirus infection was shown in our previous studies and we proposed that the combined stimulation of Ad-reactive T cells but the AdFasL transfected APCs in the presence of high levels of FasL led to efficient and specific elimination of these Ad-reactive T cells. This led to tolerization to antigens for up to 4 weeks through inhibition of APC/antigen-reactive T cells. The present experiment demonstrates that adenovirus expression of FasL within an APC can be used after a viral-induced inflammatory response to down-modulate this inflammatory response.

We also found previously that tolerance induction by APC-AdFasL is antigen specific (20–21). The present experiments show that APC-FasL+MCMV possess significantly greater anti-inflammatory activity than APC-FasL without MCMV in the modulation of the inflammatory response after MCMV infection. This result indicates that precursors of the MCMV-stimulated T cells represent a component of the proinflammatory activity of the T cells. Activation of these T cells by MCMV antigens presented by APCs results in either upregulation of Fas or upregu-

lation of Fas apoptosis signaling and increased efficiency of apoptosis. This suggests that some of the residual T cells present during the inflammatory response after MCMV infection can react with MCMV epitopes presented by APCs present at the inflammatory sites. This is consistent with the previous deduction that accumulation of T cells in target organs after a viral infection is dependent on continued movement of T cells from the periphery into the target organ (26, 27). T cells present in the central nervous system during viral and postviral encephalomyelitis represents sequestered populations of antigen-specific cells (27). Accumulation of T cells in target organs has been proposed to occur after nonspecific migration of cells followed by proliferation and expansion, or alternatively, T cells may be induced to proliferate in the target tissue by nonspecific stimulatory pathways, such as CD2-mediated processes. This is also consistent with the lower levels of IL-2 production observed in mice treated with APC-AdFasL+MCMV compared with APC-AdFasL, suggesting that MCMV-reactive T cells contribute to the inflammatory response and are deleted by APC-AdFasL+MCMV treatment.

Interactions between the splenic macrophages, B cells and T cells, are important to the normal immune response, particularly with respect to polysaccharide antigens (28). The spleen contains marginal zone macrophages, marginal zone metallophil, and red pulp macrophages, all of which play different roles in the immune response (29–31). In addition to these endogenous macrophages, exogenous macrophages and dendritic cells have been used to enhance vaccine development (32). Intravenous injection of macrophages and dendritic cells mainly results in their accumulation in the spleen, whereas macrophages

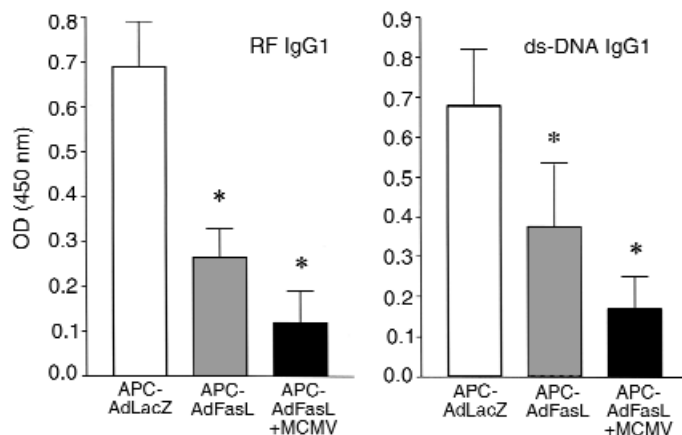


Figure 8

Decreased autoantibody production after treatment with APC-AdFasL. Four weeks after infection with MCMV, mice were treated with APC-AdLacZ control, APC-AdFasL, or APC-AdFasL+MCMV and sera was collected 4 weeks later. Production of anti-dsDNA and RF was determined on day 28 after MCMV infection of B6-*gld/gld* mice. * $P < 0.05$, compared with control treatment group.

injected subcutaneously preferentially home to draining lymph nodes. This is consistent with the present results that intravenous administration of macrophages labeled with GFP produced by an adenovirus primarily home to the spleen. The macrophage colocalizes with regions of high apoptosis and high numbers of CD3⁺ T cells. The spleen has previously been shown to be necessary for production of T cells that lead to lymphoproliferation and autoimmunity (33). In addition, splenectomy prevents development of autoantibodies in Fas-deficient *lpr* and FasL-deficient *gld/gld* mice. Analysis of T-cell traffic in the spleen indicates that fluorescent-labeled lymphocytes injected intravenously initially accumulate in the marginal zone and are associated with a layer of marginal zone macrophages (29–31). We propose that APC-FasL that are injected intravenously migrate to the marginal zone of the spleen. These macrophages are ideally located to interact with circulating T cells that enter the spleen at the marginal zone and encounter these macrophages.

Acknowledgments

The authors thank J. Palmer for her excellent assistance during the studies, F. Hunter for expert review of the manuscript, and L. Flurry for expert secretarial assistance. This work was supported in part by a VA Career Development and Merit Review Award, grants from the National Institutes of Health (NIH; NO1-AR-62224, R01-AI-42900, and R01 AI30744), a grant from Sankyo, Inc. Further support was provided by a grant from the Health Service, National Institute of Allergy and Infectious Diseases, NIH (NO1-AI-65290 to E.R. Kern). M. Fleck was supported by a grant from the Deutsche Forschungsgemeinschaft. T. Zhou is supported by a grant from the Arthritis Foundation and by a grant from the NIH (5R03AR44982). H.-C. Hsu is supported by a grant from the Arthritis Foundation.

1. Rothstein, T.L., et al. 1995. Protection against Fas-dependent Th1-mediated apoptosis by antigen receptor engagement in B cells. *Nature*. **374**:163–165.
2. Alderson, M.R., et al. 1995. Fas ligand mediates activation-induced cell death in human T lymphocytes. *J. Exp. Med.* **181**:71–77.
3. Ju, S.T., et al. 1995. Fas (CD95)/FasL interactions required for programmed cell death after T-cell activation. *Nature*. **373**:444–447.
4. Van Parijs, L., Ibraghimov, A., and Abbas, A.K. 1996. The roles of costimulation and Fas in T cell apoptosis and peripheral tolerance. *Immunity*. **4**:321–328.
5. Kiener, P.A., et al. 1997. Differential induction of apoptosis by Fas-Fas ligand interactions in human monocytes and macrophages. *J. Exp. Med.* **185**:1511–1516.
6. Dhein, J., Walczak, H., Baumler, C., Debatin, K.M., and Krammer, P.H. 1995. Autocrine T-cell suicide mediated by APO-1/(Fas/CD95). *Nature*. **373**:438–441.
7. Brunner, T., et al. 1995. Cell-autonomous Fas (CD95)/Fas-ligand interaction mediates activation-induced apoptosis in T-cell hybridomas. *Nature*. **373**:441–444.
8. Lenardo, M.J. 1996. Fas and the art of lymphocyte maintenance. *J. Exp. Med.* **183**:721–724.

9. Watanabe Fukunaga, R., Brannan, C.I., Copeland, N.G., Jenkins, N.A., and Nagata, S. 1992. Lymphoproliferation disorder in mice explained by defects in Fas antigen that mediates apoptosis. *Nature*. **356**:314–317.
10. Wu, J., Zhou, T., He, J., and Mountz, J.D. 1993. Murine autoimmune disease due to integration of an endogenous retrovirus in an apoptosis gene. *J. Exp. Med.* **178**:461–468.
11. Adachi, M., Watanabe Fukunaga, R., and Nagata, S. 1993. Aberrant transcription caused by the insertion of an early transposable element in an intron of the Fas antigen gene of *lpr* mice. *Proc. Natl. Acad. Sci. USA*. **90**:1756–1760.
12. Chu, J.L., Drappa, J., Parnassa, A.P., and Elkon, K.B. 1993. The defect in Fas mRNA expression in MRL/*lpr* mice is associated with insertion of the retrotransposon, ETn. *J. Exp. Med.* **178**:723–730.
13. Takahashi, T., et al. 1994. Generalized lymphoproliferative disease in mice, caused by a point mutation in the Fas ligand. *Cell*. **76**:969–976.
14. Lynch, D.H., et al. 1994. The mouse Fas ligand gene is mutated in *gld* mice and is part of a TNF family gene cluster. *Immunity*. **1**:131–136.
15. Cohen, P., and Eisenberg, A. 1992. Autoimmune *lpr* and *gld* mice. *Annu. Rev. Immunol.* **9**:243–265.
16. Nagata, S., and Suda, T. 1995. Fas and Fas ligand: *lpr* and *gld* mutations. *Immunol. Today*. **16**:39–43.
17. Fleck, M., Kern, E.R., Zhou, T., Lang, B., and Mountz, J.D. 1998. Murine cytomegalovirus induces a Sjogren's syndrome-like disease in C57Bl/6-*lpr/lpr* mice. *Arthritis Rheum.* **41**:217–284.
18. Fleck, M., et al. 1998. Apoptosis mediated by Fas but not tumor necrosis factor receptor 1 prevents chronic disease in mice infected with murine cytomegalovirus. *J. Clin. Invest.* **102**:1431–1443.
19. Zhang, H.G., et al. 1998. Application of a Fas ligand encoding a recombinant adenovirus vector for prolongation of transgene expression. *J. Virol.* **72**:2483–2490.
20. Zhang, H.G., et al. 1999. Induction of specific T cell tolerance by Fas ligand-expressing antigen-presenting cells. *J. Immunol.* **162**:1423–1430.
21. Zhang, H.G., et al. 1998. Induction of specific T-cell tolerance by adenovirus-transfected, Fas ligand-producing antigen-presenting cells. *Nat. Biotechnol.* **16**:1045–1049.
22. Zhang, H.G., et al. 1998. Inhibition of tumor necrosis factor alpha decreases inflammation and prolongs adenovirus gene expression in lung and liver. *Hum. Gene Ther.* **9**:1875–1884.
23. Yoshida, H., et al. 1995. Induction of apoptosis of T cells by infecting mice with murine cytomegalovirus. *J. Virol.* **69**:4769–4775.
24. Mori, T., Ando, K., Tanaka, K., Ikeda, Y., and Koga, Y. 1997. Fas-mediated apoptosis of hematopoietic progenitor cells in mice infected with murine cytomegalovirus. *Blood*. **89**:3565–3573.
25. Tam, P.E., and Messner, R.P. 1996. Genetic determinants of susceptibility to coxsackievirus B1-induced chronic inflammatory myopathy: effects of host background and major histocompatibility complex genes. *J. Lab. Clin. Med.* **128**:279–289.
26. Kinne, R.W., et al. 1995. Long-term amelioration of rat adjuvant arthritis following systemic elimination of macrophages by clodronate-containing liposomes. *Arthritis Rheum.* **38**:1777–1790.
27. Hafler, D.A., and Weiner, H.L. 1987. T cells in multiple sclerosis and inflammatory central nervous system diseases. *Immunol. Rev.* **100**:307–332.
28. Lyons, A.B., and Parish, C.R. 1995. Are murine marginal-zone macrophages the splenic white pulp analog of high endothelial venules? *Eur. J. Immunol.* **25**:3165–3172.
29. Seiler, P., et al. 1997. Crucial role of marginal zone macrophages and marginal zone metallophilic cells in the clearance of lymphocytic choriomeningitis virus infection. *Eur. J. Immunol.* **27**:2626–2633.
30. Eloranta, M.L., and Alm, G.V. 1999. Splenic marginal metallophilic macrophages and marginal zone macrophages are the major interferon-alpha/beta producers in mice upon intravenous challenge with herpes simplex virus. *Scand. J. Immunol.* **49**:391–394.
31. Martin, F., and Kearney, J.F. 1999. CD21^{high} IgM^{high} splenic B cells enriched in the marginal zone: distinct phenotypes and functions. *Curr. Top. Microbiol. Immunol.* **246**:45–50.
32. Eggert, A.A., et al. 1999. Biodistribution and vaccine efficiency of murine dendritic cells are dependent on the route of administration. *Cancer Res.* **59**:3340–3345.
33. Smathers, P.A., Santoro, T.J., Chused, T.M., Reeves, J.P., and Steinberg, A.D. 1984. Studies of lymphoproliferation in MRL-*lpr/lpr* mice. *J. Immunol.* **133**:1955–1961.